JOURNAL OF Materials CHEMISTRY

Hydrothermal synthesis and structures of the new open-framework uranyl silicates $Rb_4(UO_2)_2(Si_8O_{20})$ (USH-2Rb), $Rb_2(UO_2)(Si_2O_6)\cdot H_2O$ (USH-4Rb) and $A_2(UO_2)(Si_2O_6)\cdot 0.5H_2O$ (USH-5A; A = Rb, Cs)

Jin Huang, Xiqu Wang and Allan J. Jacobson*

Department of Chemistry and Materials Research Science and Engineering Center, University of Houston, Houston, TX 77204-5003, USA. E-mail: ajjacob@uh.edu

Received 9th September 2002, Accepted 12th November 2002
First published as an Advance Article on the web 16th December 2002

Four new open-framework alkali metal uranyl silicates, $Rb_4(UO_2)_2(Si_8O_{20})$ (USH-2Rb), $Rb_2(UO_2)(Si_2O_6)\cdot H_2O$ (USH-4Rb), and $A_2(UO_2)(Si_2O_6)\cdot 0.5H_2O$ (USH-5A; A = Rb, Cs), have been prepared hydrothermally at 245 °C. The structures of USH-2, -4, and -5 contain UO_6 tetragonal bipyramidal units connected by double chains, 4-membered rings, and single chains of SiO_4 tetrahedra, respectively. The compounds have been characterized by single crystal X-ray diffraction, scanning electron microscopy, UV-vis and infrared spectroscopy, and thermogravimetric analysis.

Introduction

The contemporary interest in compounds with open framework structures constructed from more than one polyhedral building unit (octahedra and tetrahedra, for example) reflects their importance as molecular sieves, ion-exchangers, sensors, and catalysts.[1–5] One common synthetic approach to obtain structures of this type is to combine an MO_4 (M = P, As, Si, Ge) tetrahedron and a transition metal oxyanion with a different geometry.[6] The introduction of a transition metal building unit directly into the framework can result in unusual and useful catalytic properties.[7] Much recent work has focused on the synthesis of transition metal and actinide phosphates,[1,8,9] but transition metal silicates are of increasing interest because of their generally greater stability than systems based on phosphates. Some compounds, such as the synthetic titanium silicate materials, have been used in commercial applications.[10–13] Our recent synthetic studies of transition metal silicates have led to the discovery of a series of vanadium silicates (VSH-*n*A†) with both open-framework and microporous structures that are based on cross-linking layers of silicate tetrahedra with $V^{IV}O^{2+}$ bridging units.[14–16] We have extended the approach that we developed for the VSH-*n* compounds by replacing the VO^{2+} cation with $U^{VI}O_2{}^{2+}$ as the bridging transition metal species and developed a new series of compounds, the USH-*n*A series, that contain connected silicate chains or rings, in addition to layers.

We note that framework structures containing U(VI) combined with other anions are structurally quite diverse and their properties have been studied previously.[17–20] Many uranium silicate phases have been found as minerals, though only a few synthetic examples have been reported.[18,20–22] Previously, we reported the synthesis and structures of two new uranyl silicates, $Na_2(UO_2)(Si_4O_{10})\cdot 2.1H_2O$ (USH-1) and $RbNa(UO_2)(Si_2O_6)\cdot H_2O$ (USH-3).[23] Both contain UO_6 tetragonal bipyramids that connect different condensed silicate units into 3-dimensional anionic networks; alkali metal ions provide overall charge balance and are located in channels in the structures, together with water molecules. In this paper, we report four additional examples of this new class of uranium silicates: $Rb_4(UO_2)_2(Si_8O_{20})$ (USH-2Rb), $Rb_2(UO_2)(Si_2O_6)\cdot H_2O$ (USH-4Rb), and $A_2(UO_2)(Si_2O_6)\cdot 0.5H_2O$ (USH-5A; A = Rb, Cs), which contain double chains, single chains, and 4-membered rings of silicate tetrahedra, respectively.

Experimental

Synthesis

All the chemicals used for the reactions were commercial reagent grade and were used as purchased. The syntheses of the USH-*n* compounds were carried out in Teflon-lined autoclaves under hydrothermal conditions at 245 °C. In all syntheses, the autoclaves were removed from the oven and cooled down in air after an appropriate reaction time. The crystals were filtered, washed with deionized water, and dried at room temperature.

Synthesis of USH-2Rb. The $Rb_4(UO_2)_2(Si_8O_{20})$ phase was synthesized by combining 0.1082 g SiO_2 (Cab-O-Sil M-5, Scintillation Grade, ACROS), 1.65 ml of 4.24 M aqueous RbOH, 0.509 g $UO_2(CH_3COO)_2\cdot 2H_2O$ (Alfa), and 4 ml of deionized H_2O (molar ratio Rb : U : Si : H_2O = 5.5 : 1 : 1.39 : 290). The mixture (pH ≈ 14) was stirred thoroughly and heated under autogeneous pressure for 7 days. The product consisted of a pale yellow solution over yellow crystals of USH-2Rb and some pale yellow and white amorphous impurity (unreacted silica). After decanting the liquid from the solid, the white solid material was removed by washing with 1.5 M RbOH solution and then water. Crystals (yellow polyhedra) were obtained with a yield of ~40% based on U.

Synthesis of USH-5A (A = Rb, Cs). The $A_2(UO_2)(Si_2O_6)\cdot 0.5H_2O$ (A = Rb, Cs) phases were prepared by combining 0.2545g SiO_2 (Cab-O-Sil M-5, Scintillation Grade, ACROS), 1.65 ml of 4.24 M RbOH or CsOH, 0.1080 g $UO_2(CH_3COO)_2\cdot 2H_2O$ (Alfa), and 2.7 ml of deionized H_2O [molar ratio Rb(Cs) : U : Si : H_2O = 11.7(11.7) : 1 : 3 : 340]. The mixture (pH ≈ 14) was stirred thoroughly and heated under autogeneous pressure for 7 days. The products consisted of clear solutions over yellow polyhedra of USH-5A and small amounts of a

---

†We use the notation MSH-*n*A (metal silicate Houston) to identify specific compounds, where *n* is the series number and A is the non-framework cation. Thus, VSH-*n* and USH-*n* refer to the vanadium silicate and the uranium silicate frameworks, respectively.

DOI: 10.1039/b208787c

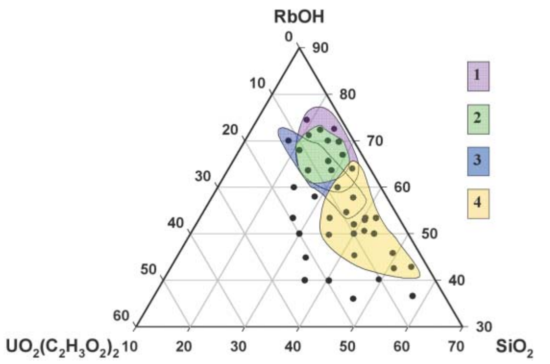

Fig. 1 Composition triangle diagram for syntheses in the system RbOH–UO$_2$(C$_2$H$_3$O$_2$)$_2$–SiO$_2$. The points show the specific reactions and the regions where specific product phases are formed: 1, USH-5Rb; 2, USH-4Rb; 3, USH-2Rb; 4, unknown phase(s).

white amorphous impurity (unreacted silica). The small amounts of impurity can be easily removed by washing. Reactions with both Rb and Cs gave light yellow polyhedral crystals with yields of approximately 80% based on U.

Synthesis of USH-4Rb. The Rb$_2$(UO$_2$)(Si$_2$O$_6$)·H$_2$O phase was originally obtained from a reaction where all three phases (USH-2Rb, -4Rb, and -5Rb) were found to coexist in final product. USH-4Rb was also frequently observed during a systematic survey of the influence of composition on the final reaction products in the RbOH–UO$_2$(CH$_3$COO)$_2$·2H$_2$O–SiO$_2$ system (see Fig. 1 and Results and discussion). However, in all reactions, USH-4Rb was always found together with either USH-2Rb or -5Rb. Fortunately, USH-4Rb crystals can be manually separated from USH-2Rb and -5Rb because of their different crystal shapes; USH-4Rb forms long needle-like crystals distinctly different in morphology from the polyhedral crystals of USH-2Rb and -5Rb (see Fig. 2).

Crystal structure determination

The crystal structures were determined from single crystal X-ray diffraction data. Crystals were mounted on glass fibers and analyzed on a Siemens SMART platform diffractometer fitted with a 1K CCD area detector and graphite-monochromatized Mo-K$_\alpha$ radiation (λ = 0.71073 Å) at 293 K. A hemisphere of data (1271 frames at 5 cm detector distance) was collected for each phase using a narrow-frame method with scan widths of 0.30° in ω and an exposure time of 30–40 s frame^{-1}. The data were integrated using the Siemens SAINT program.[24] The program SADABS was used for the absorption correction.[25] The structures were solved and refined using the SHELXTL program.[26] The crystallographic data and refinement details are summarized in Table 1. Selected bond lengths for USH-2Rb, -4Rb, and -5Rb are given in Tables 2, 3, and 4, respectively.

CCDC reference numbers 193080–193083.

See http://www.rsc.org/suppdata/jm/b2/b208787c/ for crystallographic data in CIF or other electronic format.

Characterization

All synthesis products were examined with a polarizing optical microscope. Scanning electron microscope (SEM) images were recorded on a JEOL-JSM 6400/Link Isis instrument. Chemical compostions were analyzed using a JEOL 8600 electron microprobe operating at 15 KeV with a 10 µm beam diameter and a beam current of 30 nA. The measured U/Si ratios were

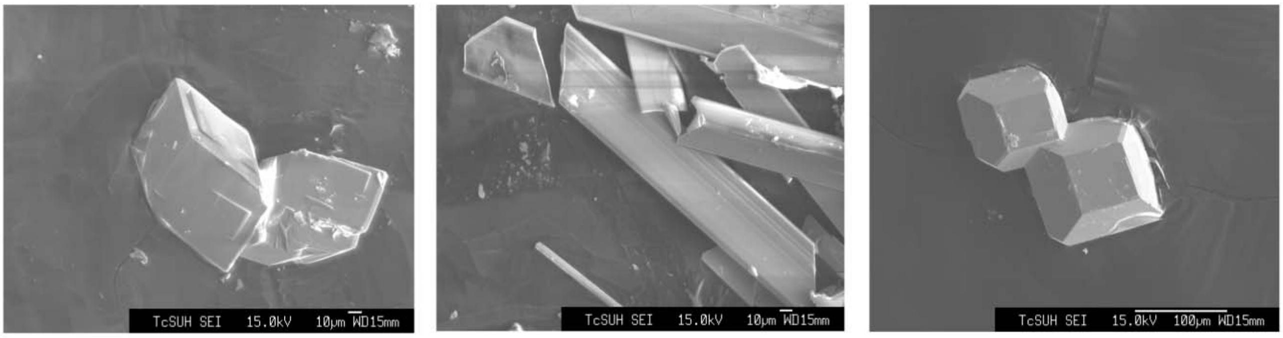

Fig. 2 SEM images of crystals of USH-2Rb, -4Rb, and -5Rb.

Table 1 Crystallographic data for Rb$_4$(UO$_2$)$_2$(Si$_8$O$_{20}$) (USH-2Rb), Rb$_2$(UO$_2$)(Si$_2$O$_6$)·H$_2$O (USH-4Rb), and A$_2$(UO$_2$)(Si$_2$O$_6$)·0.5H$_2$O (USH-5A; A = Rb, Cs)

Formula	Rb$_4$(UO$_2$)$_2$(Si$_8$O$_{20}$)	Rb$_2$(UO$_2$)(Si$_2$O$_6$)·H$_2$O	Rb$_2$(UO$_2$)(Si$_2$O$_6$)·0.5H$_2$O	Cs$_2$(UO$_2$)(Si$_2$O$_6$)·0.5H$_2$O
Formula weight	1426.66	611.166	602.158	697.04
Crystal system	Triclinic	Monoclinic	Orthorhombic	Orthorhombic
Space group	$P\bar{1}$ (no. 2)	$P2_1/n$ (no. 14)	*Pbca* (no. 61)	*Pbca* (no. 61)
a/Å	6.844(2)	7.6989(8)	14.6270(6)	15.0472(8)
b/Å	8.314(2)	20.974(2)	15.1447(7)	15.4625(8)
c/Å	11.273(3)	12.0500(12)	16.6446(7)	16.7315(8)
α/°	72.794(5)	90	90	90
β/°	88.741(5)	97.919(2)	90	90
γ/°	77.950(4)	90	90	90
V/Å^3	598.6(3)	1927.3(3)	3687.1(3)	3883.8(4)
Z	1	8	16	16
μ(Mo-K$_\alpha$)/mm^{-1}	22.09	27.15	28.38	24.37
Goodness of fit	1.053	1.015	1.183	1.034
$R_1{}^a$ [$I > 2\sigma(I)$]	0.0687	0.0519	0.0346	0.0291
$wR_2{}^a$ [$I > 2\sigma(I)$]	0.1529	0.1296	0.1037	0.0691

$^a R_1 = \Sigma||F_0| - |F_c||/\Sigma|F_0|$; $wR_2 = [\Sigma w(|F_0| - |F_c|)^2/\Sigma w|F_0|2]^{1/2}$; $w = 1/[\sigma^2(F_0{}^2) + (0.809)^2 + 24.17P]$, where $P = [\max(F_0{}^2,0) + 2F_c{}^2]/3$.

Table 2 Selected bond lengths (Å) for USH-2Rb

U–O(11)	1.822(13)	U–O(12)^{a}	1.83(2)
U–O(2)^{a}	2.274(14)	U–O(4)	2.230(13)
U–O(5)	2.22(2)	U–O(9)^{a}	2.292(13)
Si(1)–O(2)^{b}	1.578(14)	Si(1)–O(3)^{c}	1.623(14)
Si(1)–O(6)^{b}	1.640(13)	Si(1)–O(8)^{d}	1.634(14)
Si(2)–O(3)^{e}	1.637(14)	Si(2)–O(7)^{f}	1.624(14)
Si(2)–O(9)^{e}	1.595(14)	Si(2)–O(10)^{e}	1.633(14)
Si(3)–O(1)	1.65(2)	Si(3)–O(4)^{g}	1.602(13)
Si(3)–O(5)	1.63(2)	Si(3)–O(7)^{f}	1.64(2)
Si(4)–O(1)^{h}	1.584(14)	Si(4)–O(6)^{b}	1.621(13)
Si(4)–O(8)^{i}	1.61(2)	Si(4)–O(8)^{i}	1.611(14)

Symmetry codes: $^{a}-x+1,-y+1,-z$; $^{b}-x,-y+1,-z$; $^{c}x,y,z+1$; $^{d}x-1,y,z$; $^{e}x+1,y,z$; $^{f}-x+2,-y+1,-z$; $^{g}-x+1,-y+2,-z$; $^{h}-x,-y+2,-z$; $^{i}-x,-y+2,-z+1$.

Table 3 Selected bond lengths (Å) for USH-4Rb

U(1)–O(2)	1.854(8)	U(1)–O(4)	2.227(8)
U(1)–O(10)	2.250(8)	U(1)–O(13)	2.275(8)
U(1)–O(14)	1.858(8)	U(1)–O(16)	2.218(8)
U(2)–O(8)^{a}	2.276(8)	U(2)–O(9)	2.245(8)
U(2)–O(8)	2.276(8)	U(2)–O(9)^{a}	2.245(8)
U(2)–O(11)^{a}	1.838(9)	U(2)–O(11)	1.838(9)
U(3)–O(3)	1.831(8)	U(3)–O(3)^{b}	1.831(8)
U(3)–O(6)^{b}	2.237(8)	U(3)–O(6)	2.237(8)
U(3)–O(12)^{b}	2.265(8)	U(3)–O(12)	2.265(8)
Si(1)–O(6)^{c}	1.608(8)	Si(1)–O(16)^{c}	1.628(8)
Si(1)–O(7)	1.642(8)	Si(1)–O(15)^{c}	1.653(8)
Si(2)–O(4)^{d}	1.617(8)	Si(2)–O(9)^{e}	1.627(8)
Si(2)–O(5)^{f}	1.639(9)	Si(2)–O(1)^{g}	1.642(9)
Si(3)–O(12)^{g}	1.617(8)	Si(3)–O(13)	1.626(8)
Si(3)–O(15)	1.661(9)	Si(3)–O(5)	1.666(9)
Si(4)–O(1)^{h}	1.646(9)	Si(4)–O(7)	1.664(8)
Si(4)–O(8)^{i}	1.614(8)	Si(4)–O(10)^{h}	1.621(8)

Symmetry codes: $^{a}-x+2,-y,-z+2$; $^{b}-x+3,-y,-z+1$; $^{c}x-1,y,z$; $^{d}x+1/2,-y+1/2,z+1/2$; $^{e}x+1,y,z$; $^{f}x+1,y,z+1$; $^{g}x+3/2,-y+1/2,z+1/2$; $^{h}x-1/2,-y+1/2,z-1/2$; $^{i}x-1,y,z-1$.

Table 4 Selected bond lengths (Å) for USH-5Rb

U(1)–O(2)	1.826(7)	U(1)–O(3)	1.811(8)
U(1)–O(4)	2.243(8)	U(1)–O(6)	2.253(8)
U(1)–O(7)	2.244(7)	U(1)–O(11)	2.254(8)
U(2)–O(1)	1.828(7)	U(2)–O(5)	1.831(8)
U(2)–O(8)	2.207(7)	U(2)–O(9)	2.260(7)
U(2)–O(14)	2.251(7)	U(2)–O(15)	2.208(7)
Si(1)–O(12)^{a}	1.640(8)	Si(1)–O(7)^{b}	1.603(8)
Si(1)–O(10)^{c}	1.627(8)	Si(1)–O(14)^{c}	1.606(8)
Si(2)–O(11)^{b}	1.604(8)	Si(2)–O(12)^{c}	1.652(8)
Si(2)–O(15)	1.617(8)	Si(2)–O(16)	1.607(8)
Si(3)–O(6)	1.609(8)	Si(3)–O(9)	1.612(8)
Si(3)–O(10)	1.633(8)	Si(3)–O(13)^{d}	1.637(8)
Si(4)–O(4)	1.608(8)	Si(4)–O(8)^{c}	1.608(8)
Si(4)–O(13)	1.631(8)	Si(4)–O(16)^{e}	1.629(8)

Symmetry codes: $^{a}x-1/2,-y-1/2,-z+1$; $^{b}x-1/2,y,-z+1/2$; $^{c}-x+1,-y,-z+1$; $^{d}-x+3/2,y+1/2,z$; $^{e}-x+1,y-1/2,-z+1/2$.

consistent with the X-ray crystal structures. Thermogravimetric analysis (TGA) was carried out on a TA Instruments Hi-Res 2950 analyzer. Powder samples of USH-*n* were heated under flowing dry air over the temperature range 25–550 °C, with a heating rate of 3 °C min^{-1}. No rehydration experiments were performed. Powder X-ray diffraction patterns were obtained using a Scintag XDS 2000 diffractometer and Cu-K$_{\alpha}$ radiation. IR spectra were collected on a Galaxy FT-IR 500 Series spectrometer using the KBr pellet method.

UV–Vis–NIR diffuse reflectance spectra were measured with a Cary 500 spectrophotometer on powder samples at room temperature with Teflon as a reference. Absorption data were calculated from the diffuse reflectance data using the Kubelka–Munk function,[27] to allow comparison with data from the literature.

Results and discussion

Synthesis

The USH-*n* compounds were synthesized using a similar approach to that used for the synthesis of the VSH-*n* compounds. Based on our previous experience with the VSH-*n* compounds, studies of the alkali metal uranium silicate system initially focused on reactant compositions containing RbOH. Fig. 1 shows a reactant composition diagram for the RbOH–$UO_2(CH_3COO)_2{\cdot}2H_2O$–$SiO_2$ system, based on 39 experiments, which shows the regions of occurrence of different phases formed. In all of the reactions, the temperature (245 °C) and the water content (H_2O/Si molar ratio ~100) were the same. The products were identified by powder X-ray diffraction or by single crystal X-ray diffraction techniques. A similar systematic study of the corresponding CsOH system is in progress and will be reported elsewhere.

In the composition triangle shown, most of the desired phases (framework structures) are located in the region corresponding to high concentrations of RbOH and at high Si/U ratios, in part because of the greater solubility of silica at high pH. The phases present in this region consist of three identified phases: USH-2Rb, -4Rb, and -5Rb. Both USH-2Rb and -5Rb are formed at similar starting compositions, but reactant ratios were found where single-phase products can be isolated with reasonable yields (~40% for USH-2Rb and ~80% for USH-5Rb, based on U). In contrast, the reactant ratios at which USH-4Rb is observed always overlap with the conditions for formation of USH-2Rb and -5Rb. A single phase of USH-4Rb cannot be prepared at these conditions of water content and temperature. The region labeled 4 in Fig. 1 is not yet completely understood, but contains at least one apparently new phase. The products observed in the lower left region of the triangle are either amorphous or contain amorphous or known Rb uranate phases.

Structures

$Rb_4(UO_2)_2(Si_8O_{20})$ (USH-2Rb). USH-2Rb crystallizes in a triclinic system with space group $P\bar{1}$. The crystal structure is built up from interconnected UO_6 tetragonal bipyramids and branched double chains of SiO_4 tetrahedra, forming a 3-dimensional $[(UO_2)_2(Si_8O_{20})]^{4-}$ framework (Fig. 3 and 4). The framework contains narrow 6-membered channels parallel to [100]. The Rb^+ cations reside inside these channels and provide charge balance.

In this compound, one crystallographically unique UO_2^{2+} cation is coordinated by four silicate, SiO_4^{4-} anions in the equatorial plane to give a tetragonal bipyramidal coordination environment around the U(VI) center (Fig. 3). A short uranium oxygen axial bond of 1.822(13) Å [U–O(11)] is *trans* to another almost equal length bond of 1.83(2) Å [U–O(12)] with a O(11)–U–O(12) angle equal to 178.77(1)°. The four equatorial U–O bond lengths vary from 2.22(2) to 2.292(13) Å, with an average of 2.254(14) Å. Two crystallographically unique extra-framework Rb atoms are coordinated to 11 and

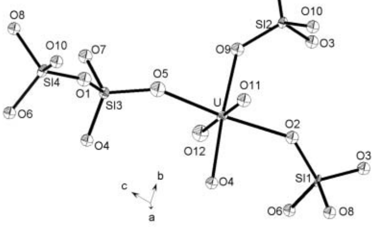

Fig. 3 Local coordination of Si and U atoms in the structure of USH-2Rb, shown with atomic displacement ellipsoids (50%).

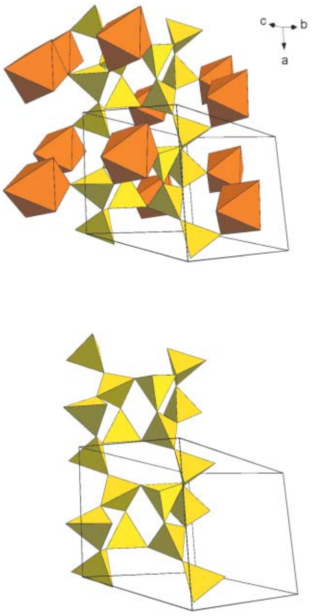

Fig. 4 The branched silicate double chain in USH-2Rb (below) and the framework structure of USH-2Rb (above), showing the connection of the UO_6 tetragonal bipyramids (orange) to the silicate double chain (yellow).

9 oxygen atoms at distances ranging from 2.931(13) to 3.633(14) Å.

The silicate anion chain, with the composition $Si_8O_{20}{}^{8-}$, forms a ''loop branched dreier double chain'', according to Liebau's classification[28] (Fig. 4). Only a small number of such branched double-chain silicate structures have been reported previously. The branched double-chain structure in USH-2Rb is similar to that found in litidionite, $Na_2K_2Cu_2(Si_8O_{20})$,[28] both having a chain periodicity of three. However, litidonnite contains only $Q^3(SiO_{3/2}O_{1/1})$ SiO_4 tetrahedra, while USH-2 has $Q^4(SiO_{4/2})$, $Q^2(SiO_{2/2}O_{2/1})$, and $Q^3(SiO_{3/2}O_{1/1})$ SiO_4 tetrahedra, in the ratio 1 : 1 : 2.

$Rb_2(UO_2)(Si_2O_6)\cdot H_2O$ (USH-4Rb). The structure of USH-4Rb is monoclinic, with space group $P2_1/n$. The 3-dimensional framework is built up from single 4-membered rings of SiO_4 tetrahedra and UO_6 tetragonal bipyramids. (Fig. 5 and 6). 10-Membered channels are observed parallel to [100]. The shortest O–O distance across the 10-membered ring is 4.869(12) Å (as measured from O to O atom centers). Water molecules and charge-balancing Rb cations are found inside the channels.

Fig. 5 shows the coordination environments of the framework cations. The structure contains three unique U^{6+} sites, all of which are have tetragonal bipyramidal geometry. The tetragonal bipyramid for U(1) has apical uranyl bond lengths of 1.854(8)–1.858(8) Å and equatorial U–O bonds of 2.218(8)–2.275(8) Å. The tetragonal bipyramids for U(2) and U(3) are centrosymmetic. The apical uranyl bonds and equatorial U–O bond ranges are 1.838(9), 1.831(8) and 2.245(8)–2.276(8), 2.237(8)–2.265(8) Å, respectively. The framework is formed by interconnection of these UO_6 tetragonal bipyramids with four neighboring 4-rings of SiO_4 tetrahedra. Extra-framework Rb^+ cations and water molecules are located in the channels in an ordered environment. The distances between the water oxygen atoms and framework oxygen atoms [O(w1)–O(8) 2.800(14), O(w2)–O(4) 2.794(14) Å] indicate relatively strong hydrogen bonding.

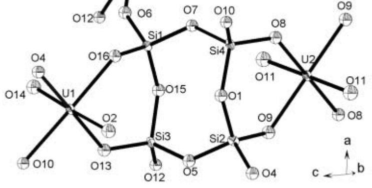

Fig. 5 Local coordination of Si and U atoms in the structure of USH-4Rb, shown with atomic displacement ellipsoids (50%).

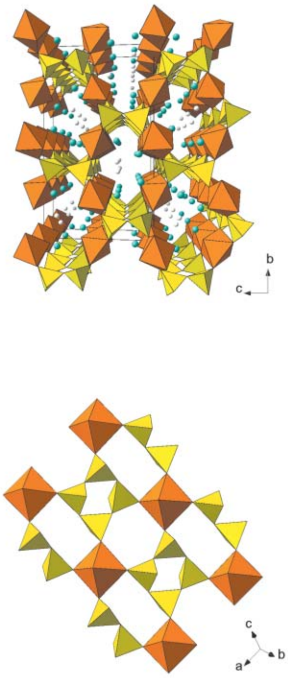

Fig. 6 (Top) A view of the structure of $Rb_2(UO_2)(Si_2O_6)\cdot H_2O$ (USH-4Rb). The blue and white circles represent Rb and water oxygen atoms, respectively, SiO_4 tetrahedra are shown in yellow and UO_6 tetragonal bipyramids in orange. (Bottom) The connection between the 4-membered SiO_4 tetrahedral rings and UO_6 tetragonal bipyramids.

The framework structure of USH-4Rb is very similar to that of previously reported $RbNa(UO_2)(Si_2O_6)\cdot H_2O$ (USH-3RbNa).[29] The two compounds both contain the same silicate 4-membered ring, but have different space groups (USH-4Rb, $P2_1/n$; USH-3RbNa, $P\bar{1}$). The difference arises from the different charge-balancing species; Rb^+ cations provide the overall neutrality for USH-4Rb, while equal numbers of Rb^+ and Na^+ ions balance the negative charge of the framework in USH-3RbNa.

$A_2(UO_2)(Si_2O_6)\cdot 0.5H_2O$ (USH-5A; A = Rb, Cs). USH-5A crystals were obtained of both Rb and Cs forms, with similar unit cell parameters (Table 1). The structural data for USH-5Rb are used as examples in the following discussion of the structure. USH-5Rb crystallizes in the orthorhombic space group *Pbca*. The framework is composed of UO_6 tetragonal bipyramids and single chains of SiO_4 tetrahedra, as shown in Fig. 7 and 8. 8-Membered ring channels and two smaller 6-membered ring channels can be observed along [001], [010], and [100] directions. Extra-framework water molecules and Rb^+ cations fill the channels.

The local coordination environments of U and Si atoms are shown in Fig. 7. Each of the two inequivalent U^{6+} ions forms short bonds with two *trans* oxygen atoms and four longer bonds to oxygen atoms that are further shared with SiO_4 tetrahedra. The apical U–O bond lengths for U(1) are 1.811(8) and 1.826(7) Å, and for U(2) are 1.828(7) and 1.831(8) Å. The longer equatorial U–O bond lengths range from 2.244(7) to 2.254(8) Å for U(1) and 2.207(7) to 2.260(7) Å for U(2).

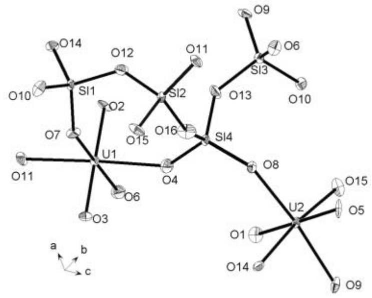

Fig. 7 Local coordination of Si and U atoms in the structure of USH-5Rb, shown with atomic displacement ellipsoids (50%).

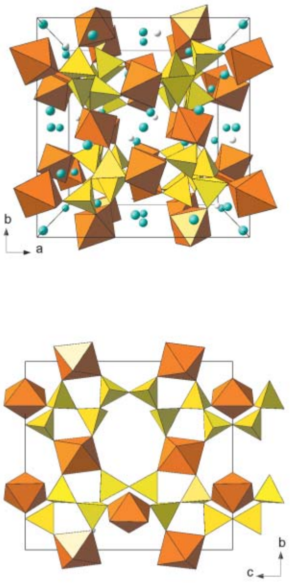

Fig. 8 (Top) A view of the structure of $Rb_2(UO_2)(Si_2O_6)\cdot 0.5H_2O$ (USH-5Rb). The blue and white circles represent Rb and water oxygen atoms, respectively, SiO_4 tetrahedra are shown in yellow and UO_6 tetragonal bipyramids in orange. (Bottom) The connection between silicate single chains and UO_6 tetragonal bipyramids in USH-5Rb.

The single chains of SiO_4 tetrahedra run parallel to the [001] direction with a periodicity of eight tetrahedra. The UO_6 tetragonal bipyramids then cross-link adjacent silicate chains to create the framework.

There are four symmetry independent Rb cation sites. The Rb(1) atom is coordinated by seven O atoms and two H_2O groups at distances ranging from 2.802(10)–3.558(8) Å. The Rb(4) atom is coordinated by eight O atoms and one H_2O group at distances ranging from 3.068(7)–3.505(8) Å, indicating somewhat weaker bonding. The Rb(2) and Rb(3) atoms, with coordination numbers of nine and eight, respectively, are not coordinated by H_2O molecules. The Rb–O distances vary from 2.952(7) to 3.519(8) Å for Rb(2) and from 2.856(7) to 3.044(8) Å for Rb(3). The water molecules are located within the 8-ring channels. Relatively strong hydrogen bonds occur between the water molecule and O(6) atoms [O(w17)···O(6) 2.70(1) Å].

Characterization

Thermal stability. Thermogravimetric analysis was used to quantify the water molecules present in the structures of USH-2, -4, and -5. The crystal structure of USH-2 indicates the complete absence of water molecules in the unit cell and the composition $Rb_4(UO_2)_2(Si_8O_{20})$. In agreement with this, thermogravimetric analysis shows no weight loss from 100 to 550 °C. The X-ray diffraction pattern of the yellow powder after thermal analysis shows that the framework of USH-2Rb remains intact after heating to 550 °C.

The thermogravimetric analysis data for USH-4Rb show a broad weight loss between ambient temperature and 550 °C, corresponding to the loss of 0.95 water molecules per formula unit. This result agrees with the estimate of 1 water molecule per formula unit from the refinement of the single crystal data. The powder X-ray diffraction pattern of USH-4Rb after TGA shows that the yellow powder is crystalline, but different from parent material. Further work is in progress to characterize this phase. Data measured from 25 to 550 °C for USH-5Cs show that between 100 and 550 °C, the sample gradually loses 1.30% in weight, corresponding to 0.5 water molecules per formula unit [USH-5Cs, $Cs_2(UO_2)(Si_2O_6)\cdot 0.5H_2O$], consistent with the results of refinement of the single crystal data. The powder X-ray diffraction pattern for the USH-5Cs sample after TGA indicates the structure remains the same, though the crystallinity is slightly less than that of the parent material.

Spectroscopy. The infrared spectra of USH-2Rb, -4Rb, and -5Rb (Fig. 9) all show Si–O and U–O stretching frequencies, as expected. The strong bands observed between $\sim$800–950 cm^{-1} can be most reasonably assigned to the stretching modes of $(UO_2)^{2+}$ ions, based on similar assignments made for other uranyl silicates.[29,30] The strong bands between $\sim$950–1200 cm^{-1} are mainly due to the stretching vibrations of the silicate group and most probably associated with the Si–O antisymmetric stretching modes. However, extensive overlap of framework silicate group bands with $(UO_2)^{2+}$ stretching vibrations complicates further assignments. The bands in the regions 1600–1700 and 3000–3600 cm^{-1} are typical for water molecules. USH-2 contains no structural H_2O, as evidenced by the absence of absorption bands in these regions, although a very broad band around 3464 cm^{-1} indicates the presence of some surface H_2O. The water bands observed for USH-5Rb are broader than for USH-4Rb, indicating that the water molecules in USH-4Rb are relatively more ordered. The sharp weak band at 1385 cm^{-1} observed for all three compounds can be attributed to the presence of SiOH groups at defect sites or at the particle surfaces.[30]

The diffuse reflectance spectra of USH-2Rb, -4Rb and -5Cs are displayed in Fig. 10. The general features observed in the three spectra are similar to those observed for the uranyl-containing compound $Pb(UO_2)(SeO_3)_2$.[31] First, there are two optical transitions at 260 and 420 nm for all three compounds, due to absorption by the uranyl centers.[28,32] Detailed assignments and interpretation were made by Denning *et al.* and Dai *et al.*, based on extensive crystal absorption spectroscopic studies of $UO_2Cl_4{}^{2-}$. For example, the bands between

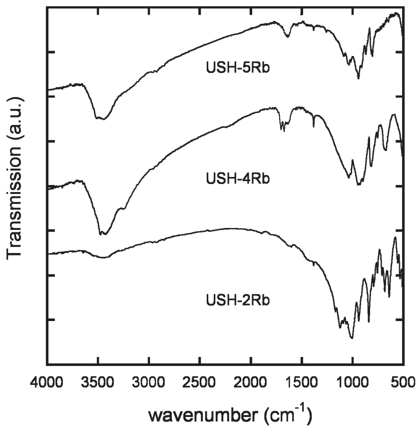

Fig. 9 Infrared spectra of USH-2Rb, -4Rb, and -5Rb.

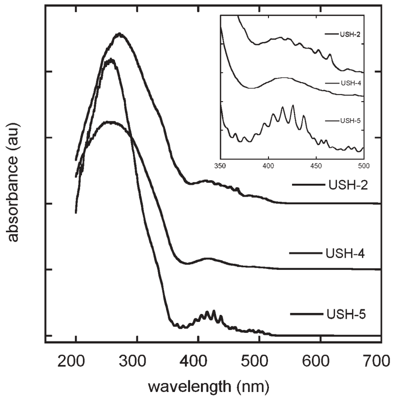

Fig. 10 UV-vis absorption spectra of USH-2Rb, -4Rb, and -5Cs. The inset shows an expansion of the 350–500 cm^{-1} region.

400–460 nm can be assigned to the transitions $\Sigma_g^+ \rightarrow \Phi_g$ and $\Sigma_g^+ \rightarrow \Delta_g$.[33,34] All of these bands show fine structure (10 nm), as can be observed in the spectrum of USH-2Rb in the band at 415 nm, but the origins of the transitions in these spectra are not yet known. The second band at ~420 nm is responsible for the pale yellow and yellow colors of the USH-*n* compounds.

Conclusions

The synthesis and structural characterization of four new alkali metal uranyl silicates USH-2Rb, -4Rb, and -5A (A = Rb, Cs) are reported. USH-5A can be prepared with Rb and Cs non-framework cations, while USH-2Rb and -4Rb can only be prepared in the Rb form. The three compounds have new open-framework structures without mineral analogs, that contain UO_6 tetragonal bipyramidal units that are connected by double chains, 4-membered rings, and single chains of SiO_4 tetrahedra in USH-2Rb, -4Rb, and -5A, respectively. Tetragonal bi-pyramidal coordination is the only geometry observed for U atoms in the USH-*n* compounds, in contrast to the coordination environments typically found in mineral structures, where seven-coordination is the norm. For example, chains of edge-shared UO_7 pentagonal bipyramids are linked by SiO_4 tetrahedra to form layers in the structures of uranophane, $Ca[UO_2]_2[SiO_3(OH)]_2\cdot 5H_2O$, sklodowskite, $Mg[UO_2]_2[SiO_4]_2\cdot 7H_2O$, boltwoodite, $K[H_3O][UO_2][SiO_4]$, and kasolite, $PbUO_2SiO_4\cdot H_2O$. The structure of weeksite, $[K_{0.62},Na_{0.38}]_2[UO_2]_2[Si_5O_{13}]\cdot 3H_2O$ is similar, but the layers are cross-linked by additional silicate terahedra, forming a 3-dimensional structure. The structures of the two forms of soddyite are exceptions to the general trend. These structures contain six-coordinate uranium atoms, but with an asymmetric geometry derived by omitting one oxygen atom from a pentagonal arrangement, in contrast to the regular tetragonal bipyramidal geometry found in the USH-*n* series.

The framework structure of USH-5A is closely related to that of NGH-5, $(C_6H_{18}N_2)\cdot Ge_{2.2}Nb_{0.8}O_{6.8}F_{1.2}$.[35] The NGH-5 structure is obtained by replacing the SiO_4 tetrahedra by GeO_4 tetrahedra and the UO_6 tetragonal bipyramids by NbO_5F distorted octahedra. Similarly, in ASU-15 $[Ge_2ZrO_6F_2\cdot(H_2DAB)H_2O]$,[36] chains of GeO_4 tetrahedra are linked into a 3-dimensional network by ZrO_4F_2 distorted octahedra.

Acknowledgements

This work was supported by the National Science Foundation under Grant DMR-0120463 and by the Robert A. Welch Foundation. This work made use of MRSEC Experimental Facilities at the University of Houston supported by the National Science Foundation under Award DMR-9632667.

References

1 A. K. Cheetham, G. Férey and T. Loiseau, *Angew. Chem., Int. Ed.*, 1999, **38**, 3268.
2 J. Rocha and M. W. Anderson, *Eur. J. Inorg. Chem.*, 2000, 801.
3 M. T. Weller, *J. Chem. Soc., Dalton Trans.*, 2000, 4227.
4 T. J. Barton and O. M. Yaghi, *Chem. Mater.*, 1999, **11**, 2633.
5 M. E. Davis, *Nature*, 2002, **417**, 813.
6 G. Perego, R. Millini and G. Bellussi, in *Molecular Sieves: Science and Technology*, ed. H. G. Karge and J. Weitkamp, Springer-Verlag, Berlin/New York, 1998, vol. 1, p. 181.
7 I. W. C. E Arends, R. A. Sheldon, M. Wallau and U Schuchardt, *Angew. Chem., Int. Ed. Engl.*, 1997, **36**, 1144.
8 R. C. Haushalter, K. G. Strohmaier and F. W. Lai, *Science*, 1989, **246**, 1289.
9 R. J. Francis, M. J. Drewitt, P. S. Halasyamani, C. Ranganathachar, D. O'Hare, W. Clegg and S. J. Teat, *Chem. Commun.*, 1998, 279.
10 M. W. Anderson, J. R. Agger, D.-P. Luigi, A. K. Baggaley and J. Rocha, *Phys. Chem. Chem. Phys.*, 1999, **1**, 2287.
11 J. Rocha, P. Brandao, J. D. Pedrosa de Jesus, A. Philippou and M. W. Anderson, *Angew. Chem., Int. Ed. Engl.*, 1997, **36**, 100.
12 X. Wang and A. J. Jacobson, *Chem. Commun.*, 1999, 973.
13 S. M. Kuznicki, V. A. Bell, S. Nair, H. W. Hillhouse, R. M. Jacubinas, C. M. Braunbarth, B. H. Toby and M. Tsapatsis, *Nature*, 2001, **412**, 720.
14 X. Wang, L. Liu and A. J. Jacobson, *Angew. Chem., Int. Ed.*, 2001, **40**, 2174.
15 X. Wang, L. Liu and A. J. Jacobson, *J. Am. Chem. Soc.*, 2002, **124**, 7812.
16 J. Huang, X. Wang, L. Liu and A. J. Jacobson, *Solid State Sci.*, 2002, **4**, 1193.
17 P. C. Burns, R. C. Ewing and F. C. Hawthorne, *Can. Mineral.*, 1997, **35**, 1551.
18 F. V. Stohl and D. K. Smith, *Am. Mineral.*, 1981, **66**, 610.
19 P. Colomban and A. Novak, *Proton Conductors*, Cambridge University Press, Cambridge, 1992.
20 P. C. Burns, R. A. Olson, R. J. Finch, J. M. Hanchar and Y. Thibault, *J. Nucl. Mater.*, 2000, **278**, 290.
21 Y. Li and P. C. Burns, *J. Nucl. Mater.*, 2001, **299**, 219.
22 J. R. Plaisier, D. J. W. Ijdo, C. D. M. Donega and G. Blasse, *Chem. Mater.*, 1995, **7**, 738.
23 X. Wang, J. Huang, L. Liu and A. J. Jacobson, *J. Mater. Chem.*, 2002, **12**, 406.
24 SAINT, version 4.05, Program for Area Detector Absorption Correction, Siemens Analytical X-ray Instruments, Madison, WI, USA, 1995.
25 G. M. Sheldrick, SADABS, Program for Siemens Area Detector Absorption Corrections, University of Göttingen, Germany, 1997.
26 G. M. Sheldrick, SHELXTL, Program for Refinement of Crystal Structures, Siemens Analytical X-ray Instruments, Madison, WI, USA, 1994.
27 W. W. Wendlandt and H. G. Hecht, *Reflectance Spectroscopy*, Interscience Publishers, New York, 1966.
28 F. Liebau, *Structural Chemistry of Silicates*, Springer-Verlag, Berlin/Heidelberg, 1985.
29 E. P. Plesko, B. E. Scheetz and W. B. White, *Am. Mineral.*, 1992, **77**, 431.
30 J. Čejka, *Rev. Mineral.*, 1999, **38**, 522.
31 P. M. Almond and T. E. Albrecht-Schmitt, *Inorg. Chem.*, 2002, **41**, 1177.
32 W. T. Carnall and H. M. Crosswhite, in *The Chemistry of the Actinide Elements*, ed. J. J. Katz, G. T. Deaborg and J. R. Morss, Chapman and Hall, London, 1986, ch. 16.
33 R. G. Denning, J. O. W. Norris, I. G. Short, T. R. Snellgrove and D. R. Woodwark, in *Lanthanide and Actinide Chemistry and Spectroscopy*, ed. N. M. Edelstein, ACS Symp. Ser. no. 131, American Chemical Society, Washington, DC, 1980, ch. 15.
34 S. Dai, Y. S. Shin, L. M. Toth and C. E. Barnes, *Inorg. Chem.*, 1997, **36**, 4900.
35 R. J. Francis and A. J. Jacobson, *Chem. Mater.*, 2001, **13**, 4676.
36 H. Li, M. Eddaoudi, J. Plevert, M. O'Keeffe and O. M. Yaghi, *J. Am. Chem. Soc.*, 2000, **122**, 12409.